



Published in final edited form as:

*Nat Neurosci.* 2010 August ; 13(8): 1027–1032. doi:10.1038/nn.2589.

## A light-gated, potassium-selective glutamate receptor for the optical inhibition of neuronal firing

Harald Janovjak<sup>1</sup>, Stephanie Szobota<sup>1</sup>, Claire Wyart<sup>1</sup>, Dirk Trauner<sup>2</sup>, and Ehud Y. Isacoff<sup>1,3</sup>

<sup>1</sup> Department of Molecular and Cell Biology, 271 Life Sciences Addition, University of California, Berkeley, CA 94720, USA

<sup>2</sup> Department of Chemistry, University of Munich, Butenandtstr. 5-13 (F4.086), D-81377 München, Germany

<sup>3</sup> Material Science Division and Physical Bioscience Division, Lawrence Berkeley National Laboratory, Berkeley, CA 94720, USA

### Abstract

Genetically targeted light-activated ion channels and pumps make it possible to determine the role of specific neurons in neuronal circuits, information processing and behavior. Here, we describe the development of a K<sup>+</sup>-selective ionotropic glutamate receptor that reversibly inhibits neuronal activity in response to light in dissociated neurons and brain slice and reversibly suppresses behavior in zebrafish. The receptor is a chimera of the pore region of a K<sup>+</sup>-selective bacterial glutamate receptor and the ligand binding domain of the light-gated mammalian kainate receptor (iGluR6/GluK2). This hyperpolarizing light-gated channel, HyLighter, is turned on by a brief light pulse at one wavelength and turned off by a pulse at a second wavelength. The control is obtained at moderate intensity. After optical activation, the photo-current and optical silencing of activity persist in the dark for extended periods. The low light requirement and bi-stability of HyLighter represent advantages for the dissection of neural circuitry.

---

Understanding the neural circuitry underlying the behavior of organisms is a fundamental challenge for both basic and clinical neuroscience. The exploration of neuronal network function has recently advanced considerably through the development of new tools for the non-invasive, reversible and precise spatio-temporal manipulation of nerve cell activity using light<sup>1, 2</sup>. “Caged” and photochromic neurotransmitter ligands first invented decades ago, and improved considerably since<sup>3</sup> were recently joined by engineered ion channels that are controlled by covalently attached synthetic photoswitched tethered ligands (PTLs)<sup>4, 5</sup>, natural photoreceptors from vertebrates<sup>6</sup> and microbes<sup>7–10</sup>, and photoswitched affinity

---

Users may view, print, copy, download and text and data- mine the content in such documents, for the purposes of academic research, subject always to the full Conditions of use: [http://www.nature.com/authors/editorial\\_policies/license.html#terms](http://www.nature.com/authors/editorial_policies/license.html#terms)

Correspondence should be addressed to E.Y.I. (ehud@berkeley.edu).

#### Author contributions

H.J. designed chimeric proteins, conducted experiments in HEK293 cells and neuronal cultures, contributed to experiments in brain slices and zebrafish, analyzed data and wrote the manuscript. S.S. conducted experiments in brain slices, analyzed data and wrote the manuscript. C.W. conducted experiments in zebrafish, analyzed data and wrote the manuscript. D.T. provided photoswitches. E.Y.I. designed chimeric proteins, analyzed data and wrote the manuscript.

labels that attach to and control native channels without the need for exogenous gene expression<sup>11</sup>.

The engineered, PTL-gated ion channels and the receptors, channels and pumps of the opsin family make it possible to control neuronal excitability in specific subsets of genetically targeted cells both *in vitro* and *in vivo*. The PTL-gated iGluR6 (GluK2) kainate receptor, LiGluR, and channelrhodopsin2 (ChR2) are cation channels that can trigger action potentials with millisecond precision<sup>5, 7</sup>. The light-driven chloride pump Halorhodopsin (HaloR) and more recently proton pumps related to bacteriorhodopsin are capable of silencing neuronal activity with millisecond resolution<sup>8–10</sup>. Rhodopsin inhibits neurons by activating native K<sup>+</sup> channels *via* a G-protein pathway, but effects on other channels and signaling proteins could also occur<sup>6</sup>. The SPARK K<sup>+</sup> channel is light-*blocked* by a PTL<sup>4</sup>. Using genetic targeting, these proteins have been successfully used to control activity in select subsets of cells in the embryonic chick<sup>6</sup>, fruit fly<sup>12–14</sup>, *C. elegans*<sup>15–18</sup>, zebrafish<sup>19–22</sup>, vertebrates and mammals (see <sup>23–25</sup> and references therein).

An intrinsic property of the light-driven pumps HaloR and bacteriorhodopsin is the requirement for continuous illumination. In addition, current magnitude depends on light intensity, which can result in the need of intensities as high as 50 mW/mm<sup>2</sup> for HaloR<sup>26</sup> and HaloR and bacteriorhodopsin inactivate partially under sustained illumination<sup>8, 10</sup>. Moreover, prolonged activation of HaloR is followed by rebound excitation<sup>19</sup>, perhaps because of efflux of the pumped Cl<sup>-</sup>. The long-term effects of proton transport in bacteriorhodopsin have not yet been evaluated. There is therefore a need for an alternative light-gated inhibitory system that can provide a sustained inhibitory conductance, without rebound excitation, that is triggered by low-intensity light.

We designed a K<sup>+</sup>-selective, light-gated ion channel. To do this, we took advantage of the modular design of mammalian glutamate receptors<sup>27–30</sup>. Ionotropic glutamate receptors (iGluRs) are cation channels that are permeant to Na<sup>+</sup> and K<sup>+</sup> (and in some cases to Ca<sup>2+</sup>) and mediate excitatory neurotransmission in all higher organisms<sup>31</sup>. The iGluRs have a common, modular architecture with a prokaryotic homologue from cyanobacterium *Synechocystis* PCC 6803, sGluR0<sup>32</sup>, with an extracellular, bi-lobed ligand binding domain (LBD) flanking a transmembrane ion channel (Fig. 1). The structures of the LBDs of several iGluRs (see <sup>33, 34</sup> and references therein), sGluR0<sup>35</sup> and of a putative glutamate receptor from *Nostoc punctiforme*<sup>36</sup> were determined using X-ray crystallography and suggested that closure of the ‘clamshell’-like LBD in all of these receptors forces the opening of the transmembrane pore (Fig. 1a, b). The pore of sGluR0 is K<sup>+</sup>-selective and its re-entrant pore loop has a GYG-amino acid motif<sup>32</sup> typical of, and homologously located to the K<sup>+</sup> channel selectivity filter. The idea that K<sup>+</sup> selectivity can exist in a prokaryotic glutamate receptor supports a functional resemblance and evolutionary connection of iGluRs and K<sup>+</sup> channels<sup>27, 29, 30</sup>. We engineered chimeric ionotropic glutamate receptors that possess the LBD of iGluR6, including the PTL attachment site that renders it light sensitive in LiGluR<sup>5</sup>, and combined this with the membrane spanning domain, and thus the pore, of sGluR0. One of the chimeras functions as a light-gated K<sup>+</sup> channel, which responds with maximal activation at low light intensity and provides the advantageous properties of sustained photoresponses in the dark and light-induced closure.

## Results

### Expression and attempted PTL agonism of sGluR0

We first asked whether the K<sup>+</sup>-selective sGluR0 could be converted into a tool for optical silencing of neuronal activity. We expressed a mammalian signal peptide modified and codon-optimized version of sGluR0 in HEK293 cells. The transfected cells had small glutamate-induced currents (peak currents of  $130 \pm 37$  pA measured at +60 mV,  $n = 5$ ). We tested if sGluR0 can be activated by a soluble test compound (the “tether model”) shown earlier to mimic the maleimide azobenzene glutamate (MAG) PTL and activate iGluR6<sup>5</sup>. No activation of sGluR0 was detected by 0.5–3mM of “tether model” (Supplementary Fig. 1). This lack of agonism is in agreement with the observation that the ligand binding motif of sGluR0 differs from that of the iGluRs and that the ligand docks in an opposite orientation, which would yield a steric clash with the “tether”<sup>35, 36</sup>. A further problem for trying to hyperpolarize cells with a light-gated sGluR0 is that sGluR0 activates very slowly (time constant of activation of ~290ms<sup>32</sup>), too slowly for the highly temporally precise inhibition of action potential firing. Taken together, the small and slowly activating currents of sGluR0 and the lack of agonism by the MAG tether model indicated that another strategy was needed to create a light-gated inhibitory channel.

### Chimeras of a light-gated LBD and the K<sup>+</sup>-selective pore

We turned to the notion of designing a K<sup>+</sup>-selective light-gated channel by combining the MAG photoswitching of the iGluR6 LBD<sup>5</sup> with the K<sup>+</sup> pore of sGluR0. A chimeric protein may combine the rapid activation of iGluR6 by glutamate and photoswitching<sup>37</sup> with the K<sup>+</sup> selectivity of sGluR0. AMPA and Kainate receptor LBDs have already been shown to gate pores (and pore-loops) of members of other iGluR families, including of the otherwise non-functional delta receptors<sup>28, 38</sup>. However, although the iGluR6 LBD was shown to gate the sGluR0 pore, and the LBD of the NR1 NMDA receptor could gate several K<sup>+</sup> channel pore-loops (not including that of sGluR0), none of these was K<sup>+</sup>-selective<sup>39</sup>, indicating that selectivity depends on more than just the K<sup>+</sup> channel pore-loop. Furthermore, experiments showed that transplanting the GYG-motif to iGluRs did not render them K<sup>+</sup>-selective<sup>40</sup>. We therefore designed an alternative set of chimeras with the hope of obtaining coupling, while preserving K<sup>+</sup> selectivity.

In the chimeric receptors different portions of the iGluR6 pore were replaced by the corresponding codon-optimized portion of the sGluR0 pore (we refer to these as “iGluR6-p0”). We aimed to transplant both transmembrane helices and the re-entrant pore-loop of sGluR0 (TM1-P-TM2, Fig. 1c), while retaining the native pore-LBD linkers of iGluR6. In the absence of crystal structures, we estimated the locations of the ends of the helices in sGluR0 and iGluR6 using sequence comparison to two K<sup>+</sup> channels with known structures, KcsA and Kv1.2, and hydrophathy analysis (Supplementary Fig. 2). Several excision sites were chosen and a total of 7 unique chimeras were generated and tested.

Our first set of chimeras, iGluR6-p0-A, B, C, D and E, varied only in the most N-terminal residues of the transplanted pore (Fig. 1c). When functionally testing chimeras in HEK293 cells we recorded large, stable glutamate-induced outward currents at –20 mV for iGluR6-

p0-A, C, D, and E (Fig. 2a). Since iGluR6-p0-C gave particularly large outward currents ( $941 \pm 239$  pA,  $n = 8$ ; Fig. 2a, b) we focused on this variant for further modifications. The iGluR6-p0-C chimera was refined into two additional variant chimeras, iGluR6-p0-F and G, in which residues in the C-terminal pore-LBD linker were replaced with residues from sGluR0. No glutamate-induced responses were detected for iGluR6-p0-F and the currents of iGluR6-p0-G ( $303 \pm 130$  pA,  $n = 8$ ) were significantly smaller than those of iGluR6-p0-C (Fig. 2a, b). The latter observation agrees with a previously proposed functional interplay of residues in this linkers and the LBD in iGluR6<sup>41</sup>.

### Photoswitching iGluR6-p0

Having found that iGluR6-p0-C was the iGluR6-p0 chimera with the largest glutamate induced currents, we added to it the MAG attachment site of the best photoswitching version of LiGluR, a leucine to cysteine substitution at position 439<sup>42</sup>. HEK293 cells expressing iGluR6-p0-C-L439C had a mean glutamate induced current of  $745 \pm 252$  pA. This final construct, termed HyLighter, had reversal potentials of glutamate-induced currents of  $-79.7 \pm 3.0$ ,  $-26.5 \pm 0.0$  and  $-1.0 \pm 2.7$  mV when the external  $K^+$  concentration was adjusted to 4, 40 and 145 mM KCl, respectively (Fig. 2c, d). Analysis of these reversal potentials with the Goldman-Hodgkin-Katz equation indicates a  $K^+ : Na^+$  permeability ratio of  $\sim 100:1$ . Current-voltage traces (Fig. 2c) exhibited the same kind of outward rectification in the presence of extracellular  $Na^+$  that was seen previously in sGluR0 and attributed to  $Na^+$  block of inward  $K^+$  current<sup>32</sup>, indicating that the sGluR0 pore maintains its character when controlled by the iGluR6 LBD in iGluR6-p0-C.

We tested the ability of HyLighter to be photo-controlled by MAG0 (Fig. 3a). After labeling with 40–60  $\mu$ M MAG0 for 20 minutes, we measured glutamate induced currents in the dark, followed by alternating illumination at 380 nm to drive isomerization to the *cis*-state of MAG0 and 500 nm to drive isomerization to the *trans*-state. The photo-currents were  $15.2 \pm 4.0$  % ( $n = 4$ ) the size of the glutamate evoked currents. Maximal photo-currents were reached at modest light intensities (Fig. 3b, c). For example, illumination with 380 nm at 0.7 mW/mm<sup>2</sup> resulted in  $95.8 \pm 1.9$  % of current achieved with maximal light intensity (14.3 mW/mm<sup>2</sup>), while illumination with 500 nm at 0.9 mW/mm<sup>2</sup> resulted in  $97.3 \pm 1.0$  % of the current seen at 20.0 mW/mm<sup>2</sup> ( $n = 4$ ). The time course of the photo-currents was intensity dependent. At maximal light intensity, half-maximal photo-currents were reached in  $28.5 \pm 2.8$  ms at 380 nm and half-maximal deactivation was reached in  $42.1 \pm 1.7$  ms at 500 nm ( $n = 4$ , Fig. 3d). The slower off-speed could be due to a stabilization of MAG0 in the *cis*-state by the binding of its glutamate end to the LBD binding pocket. Such stabilization could also slow thermal *cis* to *trans* isomerization when the glutamate end of MAG is bound in the receptor. Indeed, we detected no change in current over tens of minutes in LiGluR<sup>37</sup>. Using kinetic modeling (see Materials and Methods) and taking into account that *unbound cis*-MAG1 has a lifetime of  $\sim 25$ min<sup>37</sup> we find that a stabilization of a few kJ/mol, equivalent to the energy of a hydrogen bond, is sufficient to increase *cis*-state lifetime by one order of magnitude. This prolonged activated state in the dark combined with the ability to rapidly turn HyLighter off is a unique feature among proteins capable to hyperpolarize cells with light (see below).

### Optical suppression of neuronal firing with HyLighter

In cultured hippocampal neurons expressing HyLighter under the control of the CMV promoter, brief light pulses at 380 nm triggered photo-currents with a mean amplitude of  $92.8 \pm 13.2$  pA in whole cell voltage clamp mode (at a holding potential of  $-45$  mV,  $n = 3$ ) (Fig. 4a, top panel). In whole cell current clamp mode the same light pulse evoked hyperpolarizations of  $10.2 \pm 3.1$  mV (Fig. 4a, bottom panel). Addition of the ER-forward trafficking motif of Kir2.1<sup>43</sup>, in combination with use of the human synapsin promoter, increased currents to  $225 \pm 28$  pA and hyperpolarizations to  $15.8 \pm 2.0$  mV. Once the photo-current or photo-hyperpolarization was triggered by the 380 nm light pulse it remained constant in the dark until deactivation was induced by a light pulse at 500 nm (Fig. 4a). Photo-currents could be repeatedly activated and deactivated for hundreds of cycles without deterioration (Supplementary Fig. 3).

Action potentials triggered by the somatic injection of current through the recording pipette were suppressed by activation of HyLighter. Firing was suppressed throughout a long depolarization that triggered a train of action potentials (Fig. 4b) and in response to short bursts of action potentials during short depolarizations induced by repeated pulses of current injection (Fig. 4c). The hyperpolarization and suppression of firing persisted without decrement for extended periods (minutes) in the dark until HyLighter was rapidly turned off with a pulse of 500 nm light (Fig. 4d). HyLighter did not appear to alter the properties of the neurons in which it was expressed. HyLighter expressing cells and untransfected cells in the same preparation had similar resting potentials ( $-59.9 \pm 4.4$  mV and  $-54.3 \pm 1.8$  mV, respectively) and action potential frequencies ( $40.7 \pm 6.6$  Hz and  $37.3 \pm 1.8$  Hz, respectively,  $n = 3$ ) in response to long steps of depolarizing current injection.

Extending the technique to intact brain preparations, HyLighter was examined in cultured hippocampal slices. Slices were prepared from the hippocampi of early postnatal rats, cultured at  $34^{\circ}\text{C}$ , and transfected with HyLighter-GFP by Biolistic gene transfer. HyLighter was found to express equally well in all regions of the hippocampus (data not shown) and HyLighter-GFP protein was found to be homogeneously distributed throughout all parts of the neuron (Supplementary Fig. 4). After a brief incubation with MAG0, whole-cell recordings from individual neurons in the slice revealed that activation of HyLighter by illumination at 390 nm induced membrane hyperpolarization, and, when this took place during a train of action potentials that were evoked by depolarizing current injection, the HyLighter induced hyperpolarization robustly silenced firing (Fig. 5). The hyperpolarization induced by activation of HyLighter was strong and was sustained until HyLighter was deactivated by 500 nm light.

### Optical suppression of behavior with HyLighter

To test HyLighter function *in vivo*, we generated transgenic zebrafish expressing HyLighter and examined the effect of light on behavior. Fish expressing HyLighter-GFP under the control of a UAS promoter were crossed to fish from an enhancer trap line in which the GAL4 transcription factor is expressed in spinal cord motor neurons (Fig. 6a; line Gal4<sup>s1020t22</sup>, 44). Escape responses were triggered by a mechanical stimulus to the dish and behavior was monitored from the motions the free tail in head-embedded fish larvae. The

fish were first labeled with the MAG photoswitch at an age of 5 days post fertilization, as done earlier (Szobota, 2007; Wyart, 2009; see Methods). Bouts of mechanical stimulation were administered first in the absence of illumination, following illumination of the tail with 390 nm light ( $0.5 \text{ mW/mm}^2$ ) to activate HyLighter, and following illumination at 500 nm ( $0.5 \text{ mW/mm}^2$ ) to deactivate HyLighter. Illumination at 390 nm reduced the probability of an escape response ( $P < 0.01$ ;  $n = 14$ ; Fig. 6b) and this effect was reversed by illumination at 500 nm. The same illumination had no effect on the probability of escape responses in siblings from the same crosses which did not express HyLighter ( $P > 0.31$ ;  $n = 16$ ).

## Discussion

Light controlled systems provide many advantages for artificially manipulating biological function *in vivo* with high spatial and temporal resolution and precise control of signal strength. The ability to encode in DNA proteins that bind natural or synthetic photoswitches has made it possible to probe neuronal networks<sup>1, 2</sup> by asking how turning on and off the activity of specific cells alters information processing and behavior. While a number of light-controlled, genetically-targetable excitatory systems have been developed<sup>5, 7, 45</sup>, the only light-activated inhibitory proteins offering millisecond-resolution are pumps of the bacteriorhodopsin and HaloR families<sup>8–10</sup>.

We rationally designed a ligand-gated ion channel that is both  $\text{K}^+$ -selective and light-controlled with properties and advantages distinct from those of SPARK, HaloR and bacteriorhodopsin. Chimeras were constructed in which the transmembrane helices and re-entrant pore-loop of the  $\text{K}^+$ -selective sGluR0 were transplanted into iGluR6, and the best of these was modified for light-gating and termed HyLighter. HyLighter is light-activated, and thus not active before photoswitch conjugation. This is an advantage over light-blocked SPARK, and it minimizes the risk of compensatory changes before photoswitch conjugation. HyLighter is more sensitive to light than HaloR, reaching maximal current over a wide range of intensities to achieve substantial steady-state inhibition. HyLighter also has the unique property of converting a pulse of light into a stable hyperpolarizing current, which remains on for extended periods in the dark and then can be turned off at will by the complementary wavelength of light. This property could be valuable for behavioral experiments where incidental visual stimulation may be a confound.

HyLighter requires the delivery into the expressing tissue of the synthetic photoswitch, MAG. MAG had been earlier shown to successfully reach deep neural tissue in zebrafish, where MAG was simply added to the water to conjugate to the iGluR6 receptor clamshell and generate the excitatory light-gated LiGluR channel<sup>21</sup>, permitting an analysis of the neural basis of behavior<sup>22</sup>. We show here MAG diffusion into the zebrafish is also efficient enough to endow HyLighter with light sensitivity and thereby impart the opposite light-gated inhibition. Moreover, we show that MAG also penetrates mammalian brain slices well enough to permit as intense a light-gated inhibition as seen in dissociated neurons. Since optogenetic studies in the mammalian brain requires light delivery through implanted light sources, it may be possible to deliver MAG through the same portal that is used to place a fiber optic or a lens. Indeed, the delivery of the photoswitch under illumination could be



used to pattern photo-affinity labeling<sup>37</sup> in order to restrict receptor functionalization spatially.

## Conclusion

As done recently with the chimeric re-design of rhodopsin to control new G-protein signaling cascades<sup>46</sup>, HyLighter borrows the light gating designed into one protein and staples it onto the functional domain of another to obtain a novel light-gated functionality. HyLighter complements the existing optogenetic tools as a new, light-activated, purely hyperpolarizing ion channel. Its distinct push-pull two-wavelength design, low light requirement and unique spectral sensitivity expand possible applications for suppressing activity in specific cells within intact neural circuits, while providing temporal precision. Bi-stability allows experiments where cells can be silenced by light, and behavioral analysis carried out afterwards in ambient light, or in the dark, in the absence of a possible visual confound.

## Methods

### Synthesis of MAG-photoswitches

MAG0, MAG1 and tether model synthesis and chemical analysis were described previously<sup>5, 42</sup>.

### Protein construction and site-directed mutagenesis

A DNA segment coding for the sGluR0 pore was synthesized with mammalian codon-optimization according to the supplier's recommendation (Epoch Biolabs). The  $\alpha$ -splice isoform of iGluR6 was obtained from K. Partin (Colorado State University). An initial iGluR6-p0-variant was created by cloning the sGluR0 pore into iGluR6 using introduced sites for Bsp68I and BstEII restriction enzymes (New England Biolabs). To generate iGluR6-p0-A to G, regions flanking the sGluR0-pore were extended using polymerase chain reaction and 5'-phosphorylated oligonucleotides with corresponding overhangs. For testing, residue 32 and following of iGluR6-p0-A to G were subcloned into pcDNA3.1 containing a viral signal peptide (K. Kainanen, University of Helsinki; <sup>47</sup>). eGFP-tagged iGluR-p0-C-L439C was obtained by introducing the L439C substitution and subcloning into the pEGFP-N1 vector containing the native iGluR6 signal peptide and a WPR element for optimized expression. iGluR-p0-C-L439C-GFP-WPRE was then subcloned into pcDNA3.1 containing the human synapsin promoter. Restriction sites and point substitutions were introduced by site-directed mutagenesis (Quickchange XL, Stratagene). Residues are numbered according to the start methionine of wild-type iGluR6. Codon-optimized sGluR0 cDNA with a modified signal peptide was obtained from E. Gouaux (Oregon Health and Science University<sup>32</sup>).

### HEK293 and neuron culture and transfection

HEK293 cells were maintained in DMEM (Invitrogen) with 5% FBS (Sigma), seeded on glass coverslips coated with poly-lysine (Sigma) and transfected with glutamate receptors and eYFP in pEGFP-N1 at a ratio of 20:1 with Lipofectamine 2000 (Invitrogen).

Dissociated postnatal rat hippocampal neurons (P0–P5) were prepared and transfected using calcium phosphate as described previously<sup>21</sup>.

### **MAG conjugation to HEK293 cells and neurons**

To conjugate MAG0 in HEK293 cells, MAG0 was diluted to 40–60  $\mu\text{M}$  in extracellular recording solution containing (in mM) 145 NaCl, 4 KCl, 1 MgCl<sub>2</sub>, 2 CaCl<sub>2</sub>, 10 HEPES, pH 7.4. After illumination of MAG with 380 nm light (0.19 mW/mm<sup>2</sup>) for 2 min, cells were incubated for 20–25 min at room temperature in the dark and then rinsed with extracellular recording solution. Prior to recording, the HEK293 cells were incubated in an extracellular solution containing 0.3 mg/mL concanavalin A type VI (Sigma) to block desensitization of iGluR6. Concanavalin was applied only to HEK293 cells and never to neurons. For neurons, MAG was diluted in a solution containing (in mM) 150 NMDG-HCl, 3 KCl, 0.5 CaCl<sub>2</sub>, 5 MgCl<sub>2</sub>, 10 HEPES, 5 glucose, pH 7.4. After illumination of MAG with 380 nm light for 2 min, cells were incubated for 20–25 min at room temperature in the dark and then rinsed with extracellular recording solution.

### **Electrophysiology and light-switching in cultured cells**

Whole cell patch clamp recordings were performed with an Axopatch 200A amplifier (Molecular Devices) 36 to 72 hours after transfection for HEK cells and 2 to 5 days after transfection for neurons. Pipettes had resistances of 3 to 5 M $\Omega$  and were filled with a solution containing (in mM, for HEK cells): 140 KCl, 5 EGTA, 0.5 CaCl<sub>2</sub>, 1.0 MgCl<sub>2</sub> and 10 Hepes, pH 7.4 or (for neurons) 135 K-gluconate, 10 NaCl, 10 Hepes, 2 MgCl<sub>2</sub>, 2 MgATP, 1 EGTA, pH 7.4. For HEK cell recordings, perfusion with extracellular solution (see above) was continuous with 1.5 mM glutamate added as indicated. For reversal potential measurements, extracellular Na<sup>+</sup> was replaced by K<sup>+</sup> as mentioned in the main text. For neuron recordings, 25  $\mu\text{M}$  6,7-Dinitroquinoxaline-2,3-dione and 10mM glucose was added to the extracellular solution. Illumination was applied using a 300W wavelength switching system with 1–2 millisecond switching time (DG-4P, Sutter Instruments) connected the back illumination port of the microscope (IX70, Olympus). Light intensities were determined using a power meter (Newport). Filters for 380 and 500 nm illumination (Semrock) had bandwidths of 34 and 25 nm, respectively, and were directed to a 20X objective (Olympus) using a total reflectance mirror (Edmund Optics). Electrophysiological data was recorded with pClamp software (Molecular Devices), which was also used to automatically control the illumination device. Only neurons with a resting potential  $\sim$ –50 mV were analyzed.

### **Preparation of cultured hippocampal slices**

Hippocampi were obtained from postnatal Sprague-Dawley rats (P6–P7), cut into 400  $\mu\text{m}$  slices and cultured on 0.4  $\mu\text{m}$  Millicell culture inserts (Millipore) in Neurobasal-A medium (Gibco) supplemented with 20% horse serum, insulin, ascorbic acid, GlutaMAX (Gibco), penicillin/streptomycin, Hepes, and Ara-C. Slices were transfected one day after isolation (1 DIV) by Biolistic gene transfer using a BioRad Helios Gene Gun and gold microcarriers coated with both HyLighter-GFP-WPRE (in pcDNA3.1 containing the human synapsin promoter) and cytosolic tdTomato DNA (to aid in the visualization of the transfected cells).



## MAG conjugation and hippocampal slice electrophysiology

Electrophysiological recordings were obtained from slices on 6–9 DIV. Just prior to recording, slices were incubated at room temperature for 30 min with MAG0 (250 $\mu$ M) diluted in NMDG-labeling solution (150 NMDG-HCl, 3 KCl, 0.5 CaCl<sub>2</sub>, 5 MgCl<sub>2</sub>, 10 HEPES, 5 glucose, pH 7.4). Slices were rinsed 2x in labeling solution before recording. Whole-cell patch clamp recordings were performed on an upright Zeiss AxioExaminer using an Axopatch 200B amplifier (Molecular Devices). Pipettes had resistances of 3 to 5 M $\Omega$  and were filled with the neuron pipette solution containing (135 K-gluconate, 10 NaCl, 10 Hepes, 2 MgCl<sub>2</sub>, 2 MgATP, 1 EGTA, pH 7.4). The slices were perfused with aCSF consisting of (in mM): 119 NaCl, 2.5 KCl, 1.3 MgSO<sub>4</sub>, 1 NaH<sub>2</sub>PO<sub>4</sub>-H<sub>2</sub>O, 26.2 NaHCO<sub>3</sub>, 11 glucose, 2.5 CaCl<sub>2</sub>. The aCSF was continually circulated and bubbled with 95% O<sub>2</sub>/5% CO<sub>2</sub>. The light used for photoswitching was from a DG-4 (Sutter Instruments) coupled to the microscope and projected onto the sample through a digital micromirror device (Mosaic System, Photonic Instruments) through a 40X objective. Light intensity at the sample was approximately 20 mW/mm<sup>2</sup> at 390 nm and 40 mW/mm<sup>2</sup> at 500 nm. In many cases, the illumination area was smaller than the neuron and distal processes were not subject to photostimulation.

## Generation of stable zebrafish transgenic line

To make the UAS: iGluR-p0-C-L439C-GFP transgenic construct, the iGluR-p0-C-L439C-GFP was subcloned in between the Tol2 recognition sequences in the pT2KXIG in vector<sup>48</sup>. *Gal4<sup>s1020t</sup>* embryos<sup>22, 44</sup> were injected at the one-cell stage with a solution of 25 ng/ $\mu$ l UAS: iGluR-p0-C-L439C-GFP DNA, 50 ng/ $\mu$ l transposase mRNA and 0.04% Phenol Red. F1 embryos were screened by fluorescence and used for experiments five days post fertilization.

## MAG Labeling and photostimulation on zebrafish larvae

MAG-1 and MAG-0 were diluted to 5 mM in DMSO and preactivated by UV light (365 nm) for 5 min. The E3 medium was then added to reach the final concentration of 100  $\mu$ M MAG. Five day old larvae were bathed in the labeling solution for 30 min at 28.5°C. The larvae were then washed three times with fresh E3 medium. Following an hour recovery period, all spontaneously swimming larvae were embedded in agar and their tails were freed. The light source used for photoswitching was a DG-4 (Sutter Instruments) coupled to an upright Zeiss AxioExaminer epifluorescence microscope (the light power was 0.5 mW/mm<sup>2</sup> at 390 nm and 500 nm). Escape responses were induced by mechanical taps to the dish at a 10 s inter-stimulus interval. UV light pulses (one to five second duration) illuminating the tail were immediately followed by the mechanical stimulus. Motion of the tail was monitored under low light conditions at 60fps using a CCD camera coupled to the side port of the AxioExaminer microscope and a 5X objective. The tracking of the tail position was performed using a custom made script written in Matlab 2007 (Mathworks).

## Kinetic model

We describe MAG with a two-state model in which the high energy *cis*-state is separated from the low-energy *trans*-state by a single energy barrier. In the dark after UV illumination

the only existing reaction is the thermally activated *cis-trans* isomerization. This process can

be described by an Arrhenius-type equation<sup>49, 50</sup>,  $\frac{1}{\tau} = Ae^{-\frac{E_A}{k_B T}}$ , where  $\tau$  denotes *cis*-state lifetime,  $A$  attempt frequency ( $\approx 10^{10} \text{s}^{-1}$  for azobenzenes<sup>49, 50</sup>),  $E_A$  activation energy (i.e. height of the energy barrier) and  $k_B T$  thermal energy.  $E_A$  can be determined to be  $\approx 75 \text{kJ/mol}$  by inserting  $\tau$  of 25.47 min<sup>37</sup> into the Arrhenius equation after rearranging. This value agrees well with that of other azobenzene photoswitches<sup>49, 50</sup>. Finally, the Arrhenius equation allows estimating that increasing  $E_A$  by less than 10% (6 kJ/mol) results in a increased lifetime of one order of magnitude.

## Supplementary Material

Refer to Web version on PubMed Central for supplementary material.

## Acknowledgments

This work was supported by the NIH Nanomedicine Development Center for the Optical Control of Biological Function (SPN2EY018241), Human Frontier Science Program (RPG23-2005), a fellowship of the European Molecular Biology Organization (to H.J.) and a Marie-Curie fellowship (to C.W., the fellowship was obtained with the laboratory CNRS - UMR5020 “Neurosciences Sensorielles, Comportement Cognition”, Lyon, France). We thank K. Partin, K. Kainanen, E. Gouaux and M. Hollmann for constructs, G. Sandoz and F. Tombola for discussions, D. Fortin, T. Tracey, K. Greenberg, A. Pham, M. Soden, H. Lu, E. Warp, K. McDaniel, R. Arant and Z. Fu for technical assistance and M. Volgraf and V. Franckevicius for MAG compounds.

## References

- Herlitze S, Landmesser LT. New optical tools for controlling neuronal activity. *Curr Opin Neurobiol.* 2007; 17:87–94. [PubMed: 17174547]
- Zhang F, Aravanis AM, Adamantidis A, de Lecea L, Deisseroth K. Circuit-breakers: optical technologies for probing neural signals and systems. *Nat Rev Neurosci.* 2007; 8:577–581. [PubMed: 17643087]
- Ellis-Davies GC. Caged compounds: photorelease technology for control of cellular chemistry and physiology. *Nat Methods.* 2007; 4:619–628. [PubMed: 17664946]
- Banghart M, Borges K, Isacoff E, Trauner D, Kramer RH. Light-activated ion channels for remote control of neuronal firing. *Nat Neurosci.* 2004; 7:1381–1386. [PubMed: 15558062]
- Volgraf M, et al. Allosteric control of an ionotropic glutamate receptor with an optical switch. *Nat Chem Biol.* 2006; 2:47–52. [PubMed: 16408092]
- Li X, et al. Fast noninvasive activation and inhibition of neural and network activity by vertebrate rhodopsin and green algae channelrhodopsin. *Proc Natl Acad Sci USA.* 2005; 102:17816–17821. [PubMed: 16306259]
- Boyden ES, Zhang F, Bamberg E, Nagel G, Deisseroth K. Millisecond-timescale, genetically targeted optical control of neural activity. *Nat Neurosci.* 2005; 8:1263–1268. [PubMed: 16116447]
- Chow BY, et al. High-performance genetically targetable optical neural silencing by light-driven proton pumps. *Nature.* 2010; 463:98–102. [PubMed: 20054397]
- Han X, Boyden ES. Multiple-color optical activation, silencing, and desynchronization of neural activity, with single-spike temporal resolution. *PLoS One.* 2007; 2:e299. [PubMed: 17375185]
- Zhang F, et al. Multimodal fast optical interrogation of neural circuitry. *Nature.* 2007; 446:633–639. [PubMed: 17410168]
- Fortin DL, et al. Photochemical control of endogenous ion channels and cellular excitability. *Nat Methods.* 2008; 5:331–338. [PubMed: 18311146]
- Suh GSB, et al. Light activation of an innate olfactory avoidance response in *Drosophila*. *Curr Biol.* 2007; 17:905–908. [PubMed: 17493811]

13. Zhang W, Ge WP, Wang ZR. A toolbox for light control of *Drosophila* behaviors through Channelrhodopsin 2-mediated photoactivation of targeted neurons. *Eur J Neurosci*. 2007; 26:2405–2416. [PubMed: 17970730]
14. Schroll C, et al. Light-induced activation of distinct modulatory neurons triggers appetitive or aversive learning in *Drosophila* larvae. *Curr Biol*. 2006; 16:1741–1747. [PubMed: 16950113]
15. Franks CJ, Murray C, Ogden D, O'Connor V, Holden-Dye L. A comparison of electrically evoked and channel rhodopsin-evoked postsynaptic potentials in the pharyngeal system of *Caenorhabditis elegans*. *Invert Neurosci*. 2009; 9:43–56. [PubMed: 19294439]
16. Liu Q, Hollopeter G, Jorgensen EM. Graded synaptic transmission at the *Caenorhabditis elegans* neuromuscular junction. *Proc Natl Acad Sci USA*. 2009; 106:10823–10828. [PubMed: 19528650]
17. Liewald JF, et al. Optogenetic analysis of synaptic function. *Nat Methods*. 2008; 5:895–902. [PubMed: 18794862]
18. Nagel G, et al. Light activation of channelrhodopsin-2 in excitable cells of *Caenorhabditis elegans* triggers rapid Behavioral responses. *Curr Biol*. 2005; 15:2279–2284. [PubMed: 16360690]
19. Arrenberg AB, Del Bene F, Baier H. Optical control of zebrafish behavior with halorhodopsin. *Proc Natl Acad Sci USA*. 2009; 106:17968–17973. [PubMed: 19805086]
20. Douglass AD, Kraves S, Deisseroth K, Schier AF, Engert F. Escape behavior elicited by single, channelrhodopsin-2-evoked spikes in zebrafish somatosensory neurons. *Curr Biol*. 2008; 18:1133–1137. [PubMed: 18682213]
21. Szobota S, et al. Remote control of neuronal activity with a light-gated glutamate receptor. *Neuron*. 2007; 54:535–545. [PubMed: 17521567]
22. Wyart C, et al. Optogenetic dissection of a behavioural module in the vertebrate spinal cord. *Nature*. 2009; 461:407–410. [PubMed: 19759620]
23. Ayling OGS, Harrison TC, Boyd JD, Goroshkov A, Murphy TH. Automated light-based mapping of motor cortex by photoactivation of channelrhodopsin-2 transgenic mice. *Nat Methods*. 2009; 6:219–224. [PubMed: 19219033]
24. Lagali PS, et al. Light-activated channels targeted to ON bipolar cells restore visual function in retinal degeneration. *Nat Neurosci*. 2008; 11:667–675. [PubMed: 18432197]
25. Gradinaru V, Mogri M, Thompson KR, Henderson JM, Deisseroth K. Optical Deconstruction of Parkinsonian Neural Circuitry. *Science*. 2009; 324:354–359. [PubMed: 19299587]
26. Zhao S, et al. Improved expression of halorhodopsin for light-induced silencing of neuronal activity. *Brain Cell Biol*. 2008; 36:141–154. [PubMed: 18931914]
27. Kuner T, Seeburg PH, Guy HR. A common architecture for K<sup>+</sup> channels and ionotropic glutamate receptors? *Trends Neurosci*. 2003; 26:27–32. [PubMed: 12495860]
28. Villmann C, Strutz N, Morth T, Hollmann M. Investigation by ion channel domain transplantation of rat glutamate receptor subunits, orphan receptors and a putative NMDA receptor subunit. *Eur J Neurosci*. 1999; 11:1765–1778. [PubMed: 10215929]
29. Wo ZG, Oswald RE. Unraveling the modular design of glutamate-gated ion channels. *Trends Neurosci*. 1995; 18:161–168. [PubMed: 7539962]
30. Wood MW, VanDongen HM, VanDongen AM. Structural conservation of ion conduction pathways in K channels and glutamate receptors. *Proc Natl Acad Sci USA*. 1995; 92:4882–4886. [PubMed: 7761417]
31. Gereau, RW., IV; Swanson, G. *The Glutamate Receptors*. Vol. 1. Humana Press; Totowa, NJ: 2008.
32. Chen GQ, Cui C, Mayer ML, Gouaux E. Functional characterization of a potassium-selective prokaryotic glutamate receptor. *Nature*. 1999; 402:817–821. [PubMed: 10617203]
33. Hansen KB, Yuan H, Traynelis SF. Structural aspects of AMPA receptor activation, desensitization and deactivation. *Curr Opin Neurobiol*. 2007; 17:281–288. [PubMed: 17419047]
34. Mayer ML. Glutamate receptor ion channels. *Curr Opin Neurobiol*. 2005; 15:282–288. [PubMed: 15919192]
35. Mayer ML, Olson R, Gouaux E. Mechanisms for ligand binding to GluR0 ion channels: crystal structures of the glutamate and serine complexes and a closed apo state. *J Mol Biol*. 2001; 311:815–836. [PubMed: 11518533]

36. Lee JH, et al. Crystal structure of the GluR0 ligand-binding core from *Nostoc punctiforme* in complex with L-glutamate: structural dissection of the ligand interaction and subunit interface. *J Mol Biol.* 2008; 376:308–316. [PubMed: 18164033]
37. Gorostiza P, et al. Mechanisms of photoswitch conjugation and light activation of an ionotropic glutamate receptor. *Proc Natl Acad Sci USA.* 2007; 104:10865–10870. [PubMed: 17578923]
38. Schmid SM, Kott S, Sager C, Huelsken T, Hollmann M. The glutamate receptor subunit delta2 is capable of gating its intrinsic ion channel as revealed by ligand binding domain transplantation. *Proc Natl Acad Sci USA.* 2009; 106:10320–10325. [PubMed: 19506248]
39. Hoffmann J, Villmann C, Werner M, Hollmann M. Investigation via ion pore transplantation of the putative relationship between glutamate receptors and K<sup>+</sup> channels. *Mol Cell Neurosci.* 2006; 33:358–370. [PubMed: 17011207]
40. Hoffmann J, Gorodetskaia A, Hollmann M. Ion pore properties of ionotropic glutamate receptors are modulated by a transplanted potassium channel selectivity filter. *Mol Cell Neurosci.* 2006; 33:335–343. [PubMed: 17010644]
41. Yelshansky MV, Sobolevsky AI, Jatzke C, Wollmuth LP. Block of AMPA receptor desensitization by a point mutation outside the ligand-binding domain. *J Neurosci.* 2004; 24:4728–4736. [PubMed: 15152033]
42. Numano R, et al. Nanosculpting reversed wavelength sensitivity into a photoswitchable iGluR. *Proc Natl Acad Sci USA.* 2009; 106:6814–6819. [PubMed: 19342491]
43. Ma D, et al. Role of ER export signals in controlling surface potassium channel numbers. *Science.* 2001; 291:316–319. [PubMed: 11209084]
44. Scott EK, et al. Targeting neural circuitry in zebrafish using GAL4 enhancer trapping. *Nat Methods.* 2007; 4:323–326. [PubMed: 17369834]
45. Zemelman BV, Lee GA, Ng M, Miesenbock G. Selective photostimulation of genetically chARGed neurons. *Neuron.* 2002; 33:15–22. [PubMed: 11779476]
46. Airan RD, Thompson KR, Fenno LE, Bernstein H, Deisseroth K. Temporally precise in vivo control of intracellular signalling. *Nature.* 2009; 458:1025–1029. [PubMed: 19295515]
47. Pasternack A, et al. Alpha-amino-3-hydroxy-5-methyl-4-isoxazolepropionic acid (AMPA) receptor channels lacking the N-terminal domain. *J Biol Chem.* 2002; 277:49662–49667. [PubMed: 12393905]
48. Kotani T, Nagayoshi S, Urasaki A, Kawakami K. Transposon-mediated gene trapping in zebrafish. *Methods.* 2006; 39:199–206. [PubMed: 16814563]
49. Borisenko V, Woolley GA. Reversibility of conformational switching in light-sensitive peptides. *J Photochem Photobiol A.* 2005; 173:21–28.
50. Bunce NJ, Ferguson G, Forber CL, Stachnyk GJ. Sterically hindered azobenzenes: isolation of cis isomers and kinetics of thermal cis > trans isomerization. *J Org Chem.* 1987; 52:394–398.

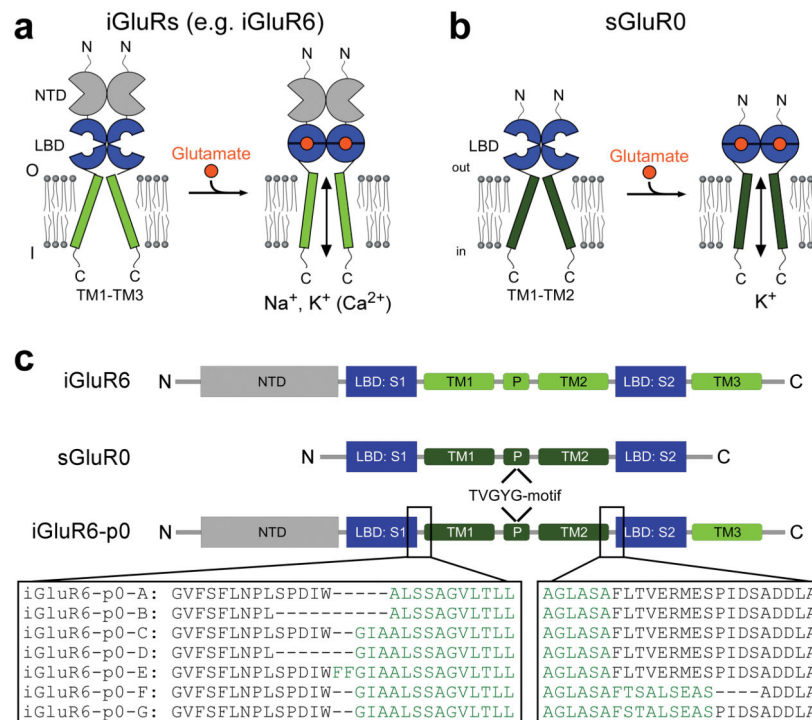


**Figure 1.** Chimeras of the iGluR6 LBD and the sGluR0  $K^+$ -selective pore. **(a)** Mammalian ionotropic glutamate receptors are modular proteins with an N-terminal domain (NTD), LBD, and transmembrane ion channel (formed by TM1, P, TM2 and TM3). Glutamate binding induces closure of the LBD and opening of a non-selective cation pore. **(b)** sGluR0 is a prokaryotic glutamate receptor that lacks an NTD and has a  $K^+$ -selective pore. **(c)** The iGluR6-p0 chimeras have the pore of sGluR0 (TM1, P with its  $K^+$  selectivity filter signature GYG-motif and TM2) inserted into iGluR6. Chimeras A-E differ at the junction between the S1 of the iGluR6 LBD and the N-terminal end of TM1 of sGluR0. Chimeras F and G use the iGluR6-p0-C S1-TM1 junction and vary in the TM2-S2 junction.

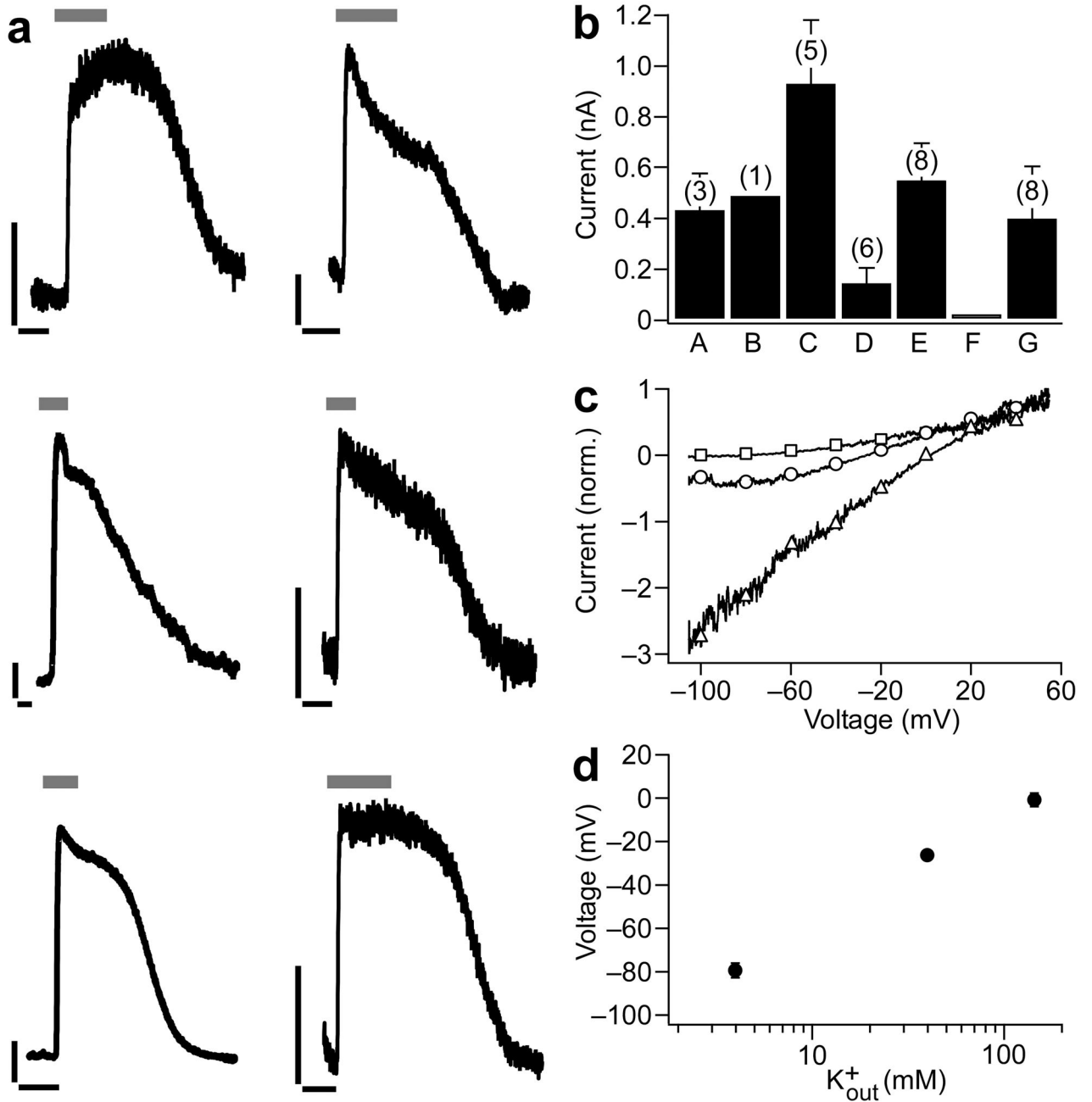


**Figure 2.** Glutamate gates  $K^+$  currents in iGluR6-p0 chimeras. **(a)** Representative, glutamate-induced outward currents recorded in whole-cell mode at  $-20$  mV after exposure to concanavalin A to block desensitization for iGluR6-p0-A (top left), iGluR6-p0-B (top right), iGluR6-p0-C (middle left), iGluR6-p0-D (middle right), iGluR6-p0-E (bottom left), iGluR6-p0-G (bottom right). For iGluR6-p0-A to G currents were observed in 60 to 100% of cells, while no currents were observed for iGluR6-p0-F and only one cell gave measurable current for iGluR6-p0-B. Black scale bars are 100 pA and 10 s. Grey horizontal bars above traces indicate perfusion of 1.5mM glutamate. **(b)** Average outward currents ( $\pm$ s.e.m.) of iGluR6-



p0 chimeras induced by 1.5mM glutamate. The largest currents are observed for iGluR6-p0-C. Number of observations in parentheses. **(c)** Leak-subtracted current for iGluR6-p0-C with added L439C mutation for photoswitch attachment in a single HEK cell during ramp changes in membrane potential (0.16 mV/ms). Extracellular solutions contained 4 mM K<sup>+</sup> and 140 mM Na<sup>+</sup> (squares), 40 mM K<sup>+</sup> and 105 mM Na<sup>+</sup> (circles) or 145 mM K<sup>+</sup> and no added Na<sup>+</sup> (triangles). Outward rectification is consistent with voltage-dependent block of inward K<sup>+</sup> current by extracellular Na<sup>+</sup>. **(d)** Reversal potentials of glutamate-induced currents shown in (c) reveal high K<sup>+</sup> selectivity of iGluR6-p0-C. S.e.m. values are the size of the symbols (n = 5 at 4 and 145 mM KCl; n = 3 at 40 mM KCl).

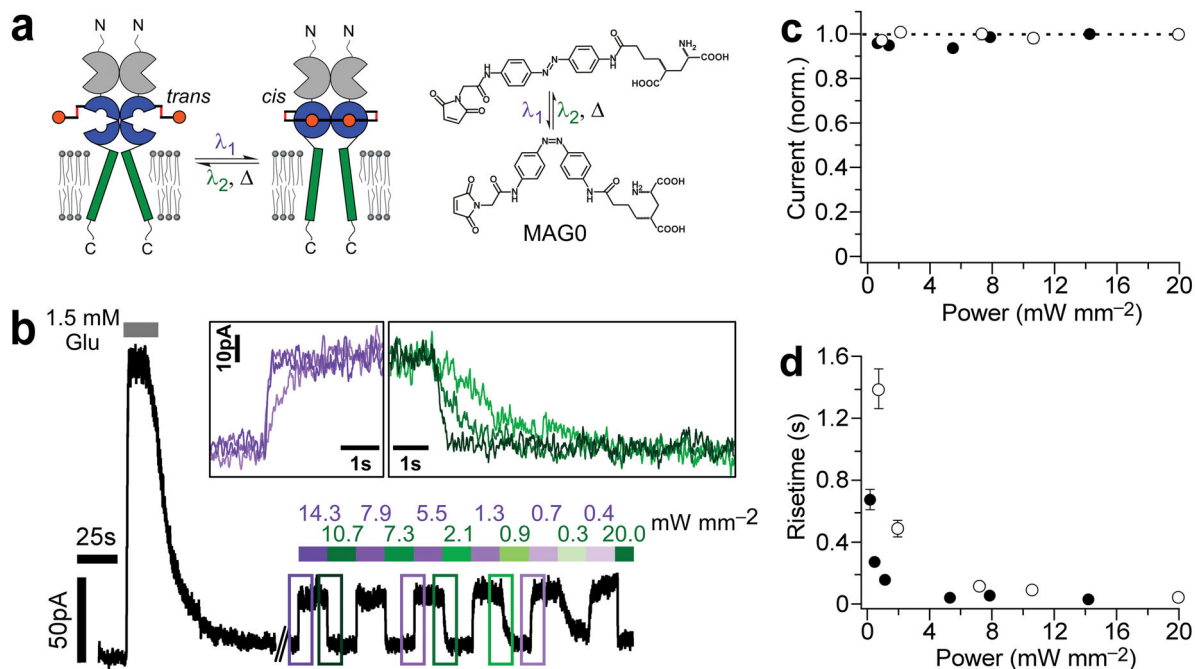


**Figure 3.**

Photo-control of K<sup>+</sup> currents. (a) The photoswitched tethered ligand MAG0 is anchored to a cysteine residue introduced into iGluR6-p0-C (L439C). Illumination at 380 nm (violet) converts the azobenzene of MAG from *trans* to *cis* and illumination at 500 nm (green) drives the reverse isomerization, thereby conferring light sensitivity by reversibly presenting/withdrawing the glutamate to/from its binding site. MAG0 consists of a glutamate, a photoisomerizable azobenzene core and a maleimide group that attaches to the cysteine. (b) Whole-cell currents at -20 mV in a HEK293 cell after labeling with MAG0 and concanavalin A. Reversible photo-currents are 17.7 % the size of glutamate evoked currents. Insets show photo-current activation and deactivation at high, medium and low light intensities. (c) Steady-state current amplitude is saturated above 1 mW/mm<sup>2</sup>. Receptor activation by UV light (filled symbols) and deactivation by green light (open symbols) are normalized to currents at highest power. (d) Reducing light intensity below 5 mW/mm<sup>2</sup> slows the rate of current activation by light.

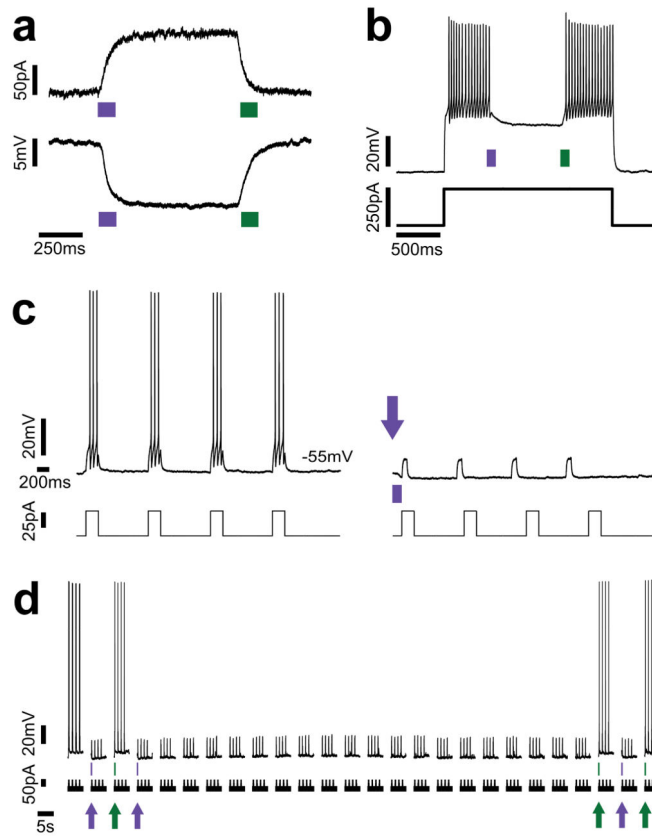


**Figure 4.**

Optical inhibition of neuronal activity. **(a)** Photo-current measured in whole-cell voltage clamp (top panel) and photo-hyperpolarization measured in whole-cell current clamp (bottom panel) recorded at  $-45$  mV membrane potential in a hippocampal neuron expressing HyLighter, following labeling with MAG. Brief (100 ms) pulses of 380 nm light (violet bars) activate the channels, which remain open in the dark and are then deactivated by 500 nm light (green bars). **(b)** Action potential firing evoked by a 250 pA pulse is silenced by 380 nm light (violet bar). The silencing persists until HyLighter is turned off by 500 nm light (green bar). **(c)** Action potential firing evoked by a 4 pulse train of 50 pA depolarizing current injections is silenced by a single light pulse. Arrow indicates brief (350 ms) illumination at 380 nm. **(d)** Inhibition of action potential firing after a single 380 nm light (violet arrows) pulse persists for seconds to minutes, until HyLighter is switching off by pulse of 500 nm light (green arrows). Four pulse depolarizing current trains given once every 7.75 seconds. Note that **(c)** and **(d)** show different neurons.



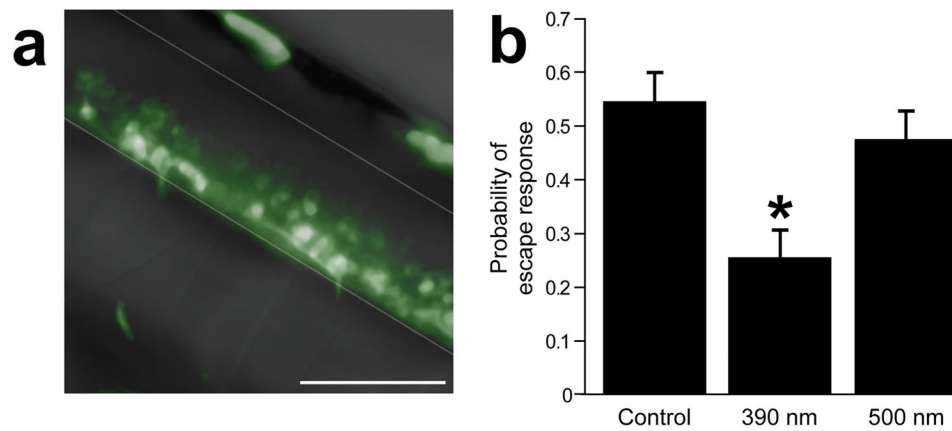


**Figure 6.**

HyLighter expressed in motoneurons of zebrafish larvae reversibly suppresses escape responses. **(a)** Expression of HyLighter-GFP (UAS: iGluR-p0-C-L439C-GFP) in the Gal4<sup>s1020t</sup> driver line, which targets motoneurons in the ventral half of the spinal cord. Ventral and dorsal limits of the spinal cord are indicated by grey lines. Rostral is on the left, caudal on the right. Scale bar is 50 $\mu$ m. **(b)** The probability of response to a mechanical stimulus (tap on the dish) is suppressed by activation of HyLighter due to illumination at 390 nm of neurons in the tail prior to the stimulus ( $P < 0.01$ ,  $n = 14$ ). The escape response recovers after illumination at 500 nm that deactivates HyLighter ( $P > 0.57$ ,  $n = 14$ ). Error bars are s.e.m.